Hossein Derakhshan, Dmytro Dizhur, Michael C. Griffith, and Jason M. Ingham

In situ out-of-plane testing of as-built and retrofitted unreinforced masonry walls

Journal of Structural Engineering, 2014; 140(6):04014022-1-04014022-12

Published at: http://dx.doi.org/10.1061/(ASCE)ST.1943-541X.0000960

Title: In-situ out-of-plane testing of as-built and retrofitted unreinforced masonry walls

Hossein Derakhshan[1], Dmytro Dizhur[2], Michael C. Griffith[3], and Jason M. Ingham[4], M.ASCE

ABSTRACT

The out-of-plane behavior of as-built and retrofitted unreinforced masonry (URM) walls was investigated by conducting in-situ static airbag tests in four buildings. The age of the buildings varied from 80 to 130 years, and all but one were constructed using clay brick masonry with timber floor and roof diaphragms. The fourth building was a reinforced concrete frame structure with pre-cracked clay block partition walls in addition to partition walls that appeared undamaged. The test program was comprised of testing five one-way vertically spanning solid URM walls from the group of three URM buildings and testing four two-way spanning URM partition walls from the reinforced concrete frame building. All walls were tested with their original support conditions, but three one-way spanning walls were additionally re-tested with modified support conditions. These additional tests allowed the effects of wall support type to be investigated, including the influence of a concrete ring beam used at the floor levels and the influence of wall to timber diaphragm anchorage by means of grouted steel rods. Several walls were next retrofitted by adding either near-surface mounted (NSM) carbon fiber reinforced polymer (FRP) strips or NSM twisted steel bars (TSB), and were then re-tested. A comparison

1 Post-doctoral Research Fellow, School of Civil, Environmental, and Mining Engineering, The University of Adelaide, SA 5005, Australia, hossein.derakhshan@adelaide.edu.au
2 Post-doctoral Research Fellow, Department of Civil & Environmental Engineering, University of Auckland, Private Bag 92019, Auckland 1010, New Zealand, ddiz001@aucklanduni.ac.nz
3 Professor, School of Civil, Environmental, and Mining Engineering, University of Adelaide, SA 5005, Australia, mcgrif@civeng.adelaide.edu.au

4 Professor, Department of Civil & Environmental Engineering, University of Auckland, Private Bag 92019, Auckland 1010, New Zealand, j.ingham@auckland.ac.nz

between the results of the tests on as-built walls and the tests conducted on retrofitted walls suggests that the simple retrofit techniques that were used are suitable for URM wall strengthening to ultimate limit state (ULS) design. The test results in two buildings highlighted significant inherent variability in masonry material properties and construction quality, and recommendations were made for the seismic assessment and retrofit of URM walls. An analytical trilinear elastic model especially useful when assessing the dynamic stability of cracked one-way spanning walls proved to satisfactorily predict the maximum wall strength, excluding those walls that developed arching action.

CE Database subject headings: Brick masonry; Walls; In situ tests; Flexural strength; Lateral loads; Axial loads; Stiffness

INTRODUCTION

While laboratory testing is suitable for a parametric wall behavior study, in-situ testing provides an opportunity to study real wall behavior in existing buildings, including the effects of actual wall support conditions. In-situ testing has also been recommended in section C7.2.3.3.4 of ASCE (2007) as an alternative method for out-of-plane URM wall seismic assessment. Calvi et al. (1996) noted that structural masonry assessment practice should be evaluated by testing, and because the construction of exact replicas of historic unreinforced masonry bearing walls is impractical, in-situ testing is frequently the most viable experimental option. Despite this notion, in-situ out-of-plane tests on full-scale URM walls have not commonly been conducted, and most available literature reports experimental programs that consist of in-situ testing for material characteristics (Corradi et al. 2003; Chiostrini et al. 2003) or non-destructive testing of masonry structures or sub-assemblies (Lopes et al. 2009; Carpinteri et al. 2005). A third approach that retains the existing masonry materials and construction quality but disrupts the support conditions and existing stress states has been to extract masonry wall panels and transport them to testing facilities (Abrams et al. 1996).

The flexural response of URM walls can be improved by using near-surface-mounted carbon fibre-reinforced-polymer (NSM FRP) strips (Griffith et al. 2013). Different wall failure modes associated with this retrofit technique have been discussed in Hamed and Rabinovitch (2010), and further studies focused on the characterization of FRP debonding as the preferred failure mode have been reported in Kashyap et al. (2012) and the references therein. In the composite NSM FRP retrofitted wall section, the FRP strips resist the tensile stresses and the masonry material resists the compression stresses. Due to the cyclic nature of the earthquake forces, the strips should therefore be inserted on both wall surfaces.

Included within this research program were walls having grouted vertical steel anchor bars (SA; Fig. 1) regularly spaced along the top edge, and a wall having a concrete ring beam (CB) placed along the top edge. The provision of steel anchor bars at the wall top edge has often been included as part of URM building retrofit projects, with the purpose being to promote wall deformations in a simply-supported mode as opposed to a cantilever mode. The presence of a concrete ring beam at building floor levels promotes arching actions that improve the wall out-of-plane behavior. As opposed to confined masonry wall construction, the wall tested with a CB support type in this research program had no vertical concrete ties.

This research program also includes walls retrofitted using either NSM FRP strips or using NSM twisted steel bars (NSM TSB). The effectiveness of the retrofit work undertaken on the tested walls is evaluated by discussing the failure modes and improvements in the wall strength and ductility.

A system of airbags were used to subject the test walls to uniform out-of-plane forces, which Priestley (1985) suggested to be a realistic representation of the out-of-plane seismic forces applied to URM walls. Details of this field study are reported, comparison is made between the predicted and measured strengths of the as-built walls, and comparison is also made between the measured strength values of the as-built and retrofitted walls. Finally, the effectiveness of the retrofit schemes is discussed.

ANALYTICAL MODEL

The two-way bending tests were conducted to proof-test wall capacity following a procedure recommended in section C7.2.3.3.4 of ASCE (2007). As recommended in that reference, the applied forces were limited to the level required by the seismic loading code and in all cases were insufficient to induce wall failure. Similarly, one of the one-way vertically spanning walls was subject to significant arching action, and the limited capacity of the in-situ test setup prevented that wall from cracking. Therefore the accuracy of relevant predictive models, e.g. Vaculik (2012) for two-way bending walls and Abrams et al. (1996) for arching action, could not be verified using the results from this in-situ test program.

The tested one-way vertically spanning URM walls had no vertical restraint to facilitate the development of arching action, and consequently the measured response of these walls was compared against a model proposed by Derakhshan et al. (2013) and another similar alternative (Fig. 2). The strength of this type of wall is relatively low and was within the capacity of the adopted test setup, such that model verification was possible for this group of walls. As discussed at the end of this section, the trilinear model is especially useful when assessing the out-of-plane dynamic stability of URM walls that have slenderness ratios exceeding values recommended in Table 7-5 of ASCE (2007). Abrams et al. (1996) proposed a model for walls that are subject to arching action from surrounding frame elements and suggested that these walls typically satisfy seismic force demand, even for regions of high seismicity. Therefore the dynamic stability of cracked walls subject to arching action is rarely required to be checked, as these walls generally satisfy strength requirements.

Using the cracked wall free body diagram and assuming rigid rocking response the theoretical wall maximum lateral resistance and instability displacement were obtained as:

$$\hat{w}_0 = \frac{Wt}{(\beta - \beta^2)h^2}[2(1-\beta) + \psi(2-\beta)] \tag{1}$$

and

$$\hat{\Delta}_{ins} = t\,\frac{1 + \psi\left(\frac{1-0.5\beta}{1-\beta}\right)}{1 + \frac{\psi}{1-\beta}} \tag{2}$$

where t, h, and β are, respectively, the wall effective thickness, total wall height, and the ratio of the height of the lower wall segment to the total wall height. When determining the effective wall thickness, the depth of mortar pointing and the thickness of weak plaster (as discussed later) should be excluded. W and ψ are respectively the wall weight per mm length and the ratio of applied overburden to wall weight. $\hat{w}_0$ and $\hat{\Delta}_{ins}$ are, respectively, the predicted wall lateral resistance and the instability displacement assuming rigid rocking as required for the rigid bilinear model shown in Fig. 2.

The ratio of the actual wall maximum lateral resistance to the theoretical equivalent value (Eq. 1) was defined as the *percentage of maximum rigid resistance* (*PMR*). The formulae were next calibrated based on laboratory airbag testing of full-scale walls, and it was found that:

$$PMR_{emp}(\%) = 83 - \frac{0.0016h}{f_j^{'}}\left(\psi + \frac{(1-\beta)(2\psi+2-\beta)}{2(1-\beta)+(2-\beta)\psi}\right)\frac{t_n}{t} \tag{3}$$

where, f'_j and t_n are, respectively, the mortar compressive strength and wall nominal thickness.

The predicted maximum wall actual lateral resistance, w_{max} (Fig. 2), is calculated as the product of the PMR_{emp} ratio from Eq. 3 and $\hat{w}_0$ from Eq. 1. The wall lateral resistance corresponding to the plateau in an idealized trilinear model (Doherty 2000), w_i, was approximated in Derakhshan et al. (2013) as being 90% of the predicted maximum wall resistance, w_{max}, and therefore,

$$w_i = 0.9 PMR_{emp}\hat{w}_0 \tag{4}$$

Similarly, simplified equations were proposed in Derakhshan et al. (2013) to calculate the predicted wall instability, Δ_{ins}, using $\hat{\Delta}_{ins}$. The trilinear model can be obtained using coordinates (0,0), (Δ_1,w_i), (Δ_2,w_i), and (Δ_{ins},0), with the two intermediate wall displacements being defined as:

$$\Delta_1 = 0.04\Delta_{ins} \tag{5}$$

and

$$\Delta_2 = (1 - 0.009PMR_{emp})\Delta_{ins} \tag{6}$$

Using time-history analyses, Griffith et al. (2003) showed that the initial stiffness of cracked out-of-plane loaded walls (i.e. w_i / Δ_1) is not a significant influencing factor when walls are assessed for dynamic stability. The acceptance criterion in these procedures (e.g. ASCE 2007, NZSEE 2006) is typically that the cracked wall displacement should not exceed 50%-60% of the wall instability displacement, Δ_{ins}. As the ratio of Δ_{ins} to Δ_1 is substantial for a cracked URM wall, the wall response can be predicted if w_i and Δ_2 in the trilinear models are reasonably accurate. Once the trilinear model has been developed, the wall displacement response can be calculated using a response spectrum method and assuming an equivalent linear system having a secant stiffness corresponding to point (Δ_2,w_i).

GENERAL DETAILS OF THE CASE STUDY BUILDINGS

The test program included three buildings with load-bearing URM walls, namely Avon House (AH; Fig. 3a; built 1884), Allen's Trade Complex (AT; Fig. 3b; built 1911), and Wintec F Block (WT; Fig. 3c; built 1917). These three buildings were constructed using clay bricks and timber floor and roof diaphragms. The testing performed in these buildings was limited to one-way vertically spanning walls. The Allen's Trade Complex building had been previously damaged in the December 2007 M6.8 Gisborne earthquake, but no visible damage was found in the tested wall. Both the Avon House building and the Wintec F Block appeared undamaged prior to testing, although the former was located in a region (Wellington, New Zealand) that is subject to high winds and high seismicity.

Tests were also conducted on single-wythe unreinforced terracotta hollow block masonry partition walls of the three-storey William Weir House (WH; Fig. 3d; built 1932), which had a reinforced concrete frame with concrete floor slabs and a timber roof. These tests were conducted with the walls loaded in a two-way bending condition and included two apparently undamaged walls and two pre-cracked partition walls. The building is located in a highly seismic region of New Zealand (Wellington), and had been subject to prior earthquakes. The 24 June 1942 Wairarapa earthquake (M7.2, Modified Mercalli in Wellington: 6 to 7 depending on ground structure) and the 02 August 1942 Wairarapa earthquake earthquake (M7, Modified Mercalli in Wellington: 6) occurred 10 years after the building had been constructed, with widespread collapse of chimneys, masonry walls and parapets into Wellington streets being reported (Downes et al. 2001). It is assumed that the cracked walls in WH was attributable to prior earthquake loading as these cracked walls had no support along their top edge and were located in the top-storey. It is also possible that even the second-storey walls had some internal cracking that was not visible.

WALL PROPERTIES

All test walls were either single-wythe or double-wythe (see Fig. 4) and had plaster finish on one or both faces as detailed in Table 1. Walls in Avon House had lime-based plaster with added horse hair (Fig. 4a) with an average thickness of 20 mm, and walls in the other test buildings had 10-15 mm thick cement-based plaster. As an exception, Wall AH3 had undergone a prior seismic upgrade by means of an applied layer of high cement content plaster on one surface, with the other wall face having the original lime-based plaster finish.

Walls subjected to one-way bending were prepared by introducing two vertical wet cuts using a concrete chainsaw, resulting in an isolated wall strip that permitted out-of-plane rocking. The final length of one-way vertically spanning walls was recorded as varying between 1170 mm and 1250 mm, as detailed in Table 1 and Fig. 5. Most walls spanned the height of a complete storey, with the exceptions being AH3 and AT. Tests were performed only on the lower parts of these walls, so that the top wall segments could be retained for the reasons explained below. AT was a lower central segment of an end gable (crown height 6500 mm from the first level timber floor, see also Fig. 3b), and the building owner wished to retain the gable end and to demolish the end wall to only the eaves level. The aforementioned vertical cuts were therefore made up to a height of 3000 mm from the timber floor, forming a continuous top support (C, Fig. 5e). This configuration resulted in the wall having an applied overburden load that was equal to the weight of the masonry column above the wall, which was calculated as 13 kN per meter length of wall. Wall AH3 was to be demolished only up to a height of 2700 mm from the wall base (storey height 3100 mm) to allow preservation of the original roof drainage details as requested by the owner. Therefore the test area was isolated from the rest of the wall by forming a lintel assembly that accommodated up to 25 mm vertical movement at the wall top (Fig. 5d). It was intended that wall vertical movements due to out-of-plane rocking be limited to 25 mm to exclude potential damage to higher elevation brickwork.

AH1 and AH2 were two similar test strips of a single partition wall, with steel plates embedded in three of the mortar joints of the wall (see Fig. 4a). The severely corroded plates were considered to not increase wall strength for the one-way bending condition.

The top horizontal edges of WH1 and WH2 was unrestrained, but the other edges were supported by either a reinforced concrete structural element or a URM flange wall (Fig. 6). These walls had cracks that were less than 1 mm open, but the cracking extended through the entire wall thickness. The existing cracking in Wall WH1 was less extensive than that shown for WH2 in Fig. 6 and was limited to three vertical cracks at middle-top of the wall and a minor diagonal crack at one base corner. Unlike WH1 and WH2, partition Walls WH3 and WH4 were restrained by a concrete beam along the top horizontal edge. Due to identical dimensions and proximity, Wall WH3 and Wall WH4 were assumed identical and tested in, respectively, the as-built and NSM FRP retrofitted condition. As discussed later, the results from testing suggested significant differences in the wall construction, e.g. thickness of plaster on the wall face subject to tension, or different levels of non-visible wall damage that prevented the effectiveness of the retrofit scheme to be measured.

Masonry pattern

The single-wythe walls had been built using a running bond, and the double-wythe walls had been constructed using a common bond pattern with header bricks located every fourth course. The double-wythe walls of AH building (Wall AH3) had only a few header bricks (Fig. 7a) and although the wall appeared to function as a single solid wall during the airbag tests, it separated into two wythes (Fig. 7b) during the ensuing demolition. This separation of wall wythes was attributed to the lack of binding header courses.

MATERIAL PROPERTIES

Material properties were determined by conducting in-situ and laboratory tests on extracted samples, with the results summarised in Table 2. The masonry density was calculated in the laboratory as 1650 kg/m^3 for the partition walls of building WH, and as 1800 kg/m^3 on average for all other walls. Masonry prism testing for building WH was conducted in the laboratory on two-block high prisms measuring approximately 330 mm × 300 mm × 95 mm (Fig. 8a), but masonry testing for the URM bearing wall buildings was conducted on three-brick high prisms. The plaster layer was removed from the samples prior to prism testing.

The masonry flexural bond strength (f'_{fb}) for building WH was derived from four point bending tests performed in the laboratory on masonry beam samples that included the plaster layer (Fig. 8b), but the strength value reported for building AH was determined on site following ASTM 1072 – 00a (ASTM 2001) after removing the plaster layer. As 50 mm mortar cube samples required for mortar testing using the procedure recommended in ASTM C780-02 (ASTM 2002) are unattainable from actual buildings, irregular mortar samples were cut into measurable cubic shapes and tested in compression. The average length, width and height of plaster samples for building WH were 26 mm, 21 mm and 26 mm respectively. The mortar samples from building WT measured on average 36 mm long × 24 mm wide × 30 mm high with little variation, and similar sizes were used for plaster and mortar testing in other buildings.

OUT-OF-PLANE TEST SETUP

The adopted test setup closely resembled that used to conduct laboratory testing as reported in Derakhshan (2011), and Fig. 9 shows a typical in-situ test setup. The test setup consisted of a backing plywood sheet with its timber supporting frame connected to the existing floor diaphragm. For one-way spanning walls, the applied force was partially distributed on the wall surface, with a commercial vinyl airbag (1100 mm × 2100 mm) with a skin thickness of 0.25 mm being positioned symmetrically against the wall surface as shown by the shaded area in Fig. 5. For two-way spanning walls, three airbags were used symmetrically against the wall surface, and the loaded area was approximately 70% (WH1), 80% (WH2), or 68% (WH3 and WH4) of the total wall surface. A low airbag inflation rate was adopted so that each half cycle took approximately 10 minutes to complete. The lateral pressure was controlled manually by adjusting the air inlet, with a typical applied force history being shown in Fig. 10. Despite recognition that a repeated semi-cyclic loading history can be less damaging than a reversed cyclic load history, the loading pattern shown in Fig. 10 was adopted due to difficulties associated with implementation of a test setup that allowed load reversals to be applied.

Out-of-plane reaction forces were transferred through either 4 (one-way spanning walls) or 6 (two-way spanning walls) 10-kN load cells from the backing frame to the supporting frame connected to the floor, and special smooth steel plates covered with a film of grease (Fig. 9a;

bottom-left) were used underneath the plywood backing frame to minimize friction losses. Wall displacements were measured using linearly variable differential transducers (LVDT) with 300 mm stroke length, and a high-speed data acquisition (DAQ) system with multiple channels was used to record the test data.

TESTING PROGRAM

As-built Tests

Eight tests were collectively performed on five as-built one-way vertically spanning walls, with three of the tests being conducted on walls with modified top supports (Table 3). The top support details that originally existed or were introduced for the purpose of a comparative study are summarised in Fig. 5. For example, test AH1-B was performed after wall testing with the original SA support conditions (AH1-A) and then removing the steel anchors from the top support details. Similarly, Test AT-B (Fig. 5f) was conducted after the as-built continuous top wall support had developed cracks during test AT-A (Fig. 5e). Finally, Wall WT was first tested (WT-A) using the as-built support conditions (CB in Table 3; see also Fig. 5g and 9a). The top concrete beam was next cut from both wall sides (Fig. 5h) so that no arching action could develop in the wall plane and the wall was re-tested by promoting a pinned support condition (WT-B). Four two-way bending tests that were conducted on four two-way spanning walls having as-built support conditions are also reported in Table 3.

Tests on Retrofitted Walls

After being tested in their as-built conditions (including tests with modified support details), several walls were retrofitted by either NSM FRP or NSM TSB methods and re-tested. Consistent with the loading pattern, the retrofit work was undertaken on one (tension) face of the wall only, but for earthquake resistance the retrofit should be undertaken on both wall faces. Table 4 lists the tests conducted on retrofitted walls and the details of the retrofit methods. Walls AH1, AH3, AT, and WT were retrofitted using the NSM FRP technique, which involved the use of one or two carbon FRP strips (see Table 4). The 15 mm wide × 1.2 mm thick strip had a Young's Modulus of 165 GPa and a mean tensile strength of 3100 MPa and was positioned into a groove that was cut into the wall surface. The groove extended vertically from top to bottom and was positioned at the wall centerline. Two part epoxy was used to bond the CFRP strip into the masonry substrate. To ensure maximum bond area the groove was entirely filled with epoxy prior to insertion of the CFRP strip. The groove was located on the non-loaded wall face, i.e. on the wall face that was subject to tensile actions, and on one of the tested walls (AH1) strain gauge transducers were mounted directly to the strip.

Details of the retrofit method undertaken on Wall AH2 are also reported in Table 4, with the technique being similar to the NSM FRP procedure discussed above but involving a slightly larger groove dimension, the use of a twisted steel bar instead of an FRP strip, and the use of a cementitious grout instead of epoxy.

TEST RESULTS

In the one-way spanning as-built walls, a crack occurred at the wall base, and the walls developed an approximately horizontal crack (Fig. 11a) at an intermediate height of βh above the wall base, with β being on average 0.56. The intermediate height crack was horizontal in all tests except test AH3-A, in which the crack crossed three brick courses. The cracking pattern in this wall was attributed to a combination of the previously mentioned high-cement-content retrofit plaster and relatively weak bricks (see Table 2 for brick compressive strength).

During the one-way spanning as-built tests a rocking mechanism was formed and walls were subjected to post-cracking displacements. The maximum post-cracking mid-height lateral displacement was limited for safety considerations to approximately 70% of the wall nominal thickness. Significant crushing was observed in the lime-based plaster on the loaded surface of walls in building AH, as shown in Fig. 11b, and the plaster was debonded from the wall surface (Fig. 11c). Plaster cracking and debonding was also observed at the base of Wall WT on the loaded wall face, despite the plaster being cement-based. The observation of plaster deterioration or spalling from the wall surface in buildings AH and WT suggested that both lime-based and cement-based plaster layers are prone to debonding, resulting in a decrease in the wall thickness at pivot points.

Subsequent testing on retrofitted walls resulted in numerous new cracks being formed in the vicinity of the inserted strip or steel bar, with the final crack pattern for one test being shown in Figs. 11d.

Walls in Building AH (with steel anchors)

AH1 and AH2 – As-built

Fig. 12a shows that significant strength degradation occurred during test AH1-A. This reduction in strength was partially attributed to the aforementioned plaster deterioration, which reduced the moment arm of the restoring wall gravitational and inertial forces. The other factor that affected the wall strength was weakening of the bond at the top support anchorages due to the large wall rotations. At the conclusion of test AH1-A the wall had experienced 7 repeated semi-cycles of large displacements, and the wall behavior reached an ultimate residual state. Steel anchors at the top support were then unbolted and test AH1-B was conducted. The latter test showed that the removal of the top anchors resulted in only a slight decrease in wall strength from the residual strength recorded at the end of test AH1-A. It was concluded that the wall anchorage increased the initial strength significantly by about 150% (0.5 kPa compared to 0.2 kPa, respectively for post-cracking peak strength and the residual strength in Fig. 12a), but that this effect sharply diminished during the repeated loading. Due to the inherent variability in this type of connection and the vulnerability of the connection to cyclic loading, it is impractical to consider the improved strength for assessment of walls with similar anchorage. However the installation of anchors is recommended as they prevent the wall from responding in a cantilever mode. The arching action that developed due to the top timber diaphragm support resulted in the residual strength of AH1 exceeding that obtained from the trilinear model, as shown in Fig. 12b. In contrast to the results for AH1, the trilinear model overestimated the strength of AH2 by about 15%. The cracking force of Wall AH2 was not captured during testing due to a test setup error, and unlike AH1, this wall was tested with TD support conditions only. As AH1 and AH2 had the same dimensions and were vertical strips of the same wall, the increased strength obtained in test AH1-B was attributed to variability in masonry material properties and quality of construction. This observation is consistent with a companion study by Lumantarna et al. (2013), which reports COV of up to 50% for in-situ material tests. Consistent with the observed degradation of plaster at the cracked joint, the trilinear force-displacement model was obtained assuming an effective wall thickness which did not include the plaster layer. However, the weight of the plaster layer was included in the calculations.

Correlation of the results from AH1-B and AH2-A with the lab-based model suggests that arching action that developed due to the timber roof support resulted in less than 30% improvement in wall strength. This additional strength is considered to be undependable when undertaking a wall assessment, as the additional strength is developed only when the wall is subjected to large lateral displacements.

AH1 and AH2 – Retrofitted

Walls AH1 and AH2 were retrofitted using, respectively, NSM FRP and NSM TSB techniques and were then re-tested (see Table 4). Both retrofit schemes resulted in a substantial increase in the wall stiffness, peak strength, and ductility capacity. Fig. 12c shows that unlike the as-built walls, the retrofitted walls retained significant stiffness as the wall lateral displacement at crack height increased up to nearly 80 mm (nearly 70% of wall nominal thickness). This absence of strength loss with displacement results in significant ductility capacity. As detailed in Table 5, the results of tests AH1-NSM FRP and AH2-NSM TSB showed improvement in the wall peak strength by, respectively, 670% and 614% when compared to the as-built walls.

The failure mode in AH1-NSM FRP was in the form of numerous visible cracks that developed within the vicinity of the CFRP strip, propagating from the wall centreline towards the top and bottom wall edges. The development of masonry cracking led to gradual debonding of the CFRP strip (see Fig. 13a for same failure mode for test WT-NSM FRP). Strip rupture, a brittle failure mode associated with the NSM FRP strengthening technique, was not observed as the peak measured stresses that developed in the strip were only 40% of that necessary to cause strip rupture. The maximum strain measured in the CFRP strip during test AH1-NSM FRP was 7500 $\mu\varepsilon$ (analogous to a tensile stress of 1240 MPa) compared to the CFRP manufacturer's suggested maximum design tensile strength of 3100 MPa. The failure mode in AH2-NSM TSB was in the form of local cracking of masonry and local bending of the TSB (Fig. 13c).

As summarised in Table 5, the results of both tests AH1-NSM FRP and AH2-NSM TSB suggest that the residual displacement is significant (nearly 15 mm; 20% maximum displacement). This observation suggests that although a URM wall strengthened using these techniques may satisfy strength requirements at the ultimate limit state, the wall loses functionality after it has been subject to large displacements.

AH3 – As-built

Fig. 12d shows the response of AH3, adjusted to exclude prior wall inelastic deformations. The response of this wall was characterised by rocking and unrestrained vertical wall deformation until the 25 mm gap (see Fig. 5g) was exceeded, after which arching action developed that resulted in a nearly 100% increase in the wall strength. When discounting arching action, the response of AH3 had good correlation with the trilinear model. Such a strength increase would not occur during earthquake loading of out-of-plane walls as the full wall length will experience comparable deformations and therefore the extent of boundary restraint present in this test would not be provided in the real scenario. The main finding of this test was that the post-cracking behavioral curve excluding arching action was in good agreement with the predictive model. Similar to the case of AH1, moderate strength degradation occurred due to deterioration of the lime-based plaster.

AH3 – Retrofitted

The NSM FRP retrofit method applied to wall AH3 led to improved wall peak strength of 440% (see Table 5 and Fig 12e) when compared with the strength of the as-built wall (excluding the increase in as-built wall strength due to arching action). The failure mode was in the form of a sudden pull-out of the top portion of the CFRP strip (Fig. 13b), precluding ductile behavior. Consequently, consideration should be given in seismic retrofit design to prevent this failure mode. Similar to test AH1–NSM FRP no strip rupture was observed, and substantial cracking occurred in the masonry wall in the vicinity of the FRP strip.

Wall AT (continuous URM wall)

AT-As-built

The strength of the one-way spanning wall AT was measured to be more than twice that obtained from the lab-based trilinear model (4.5 kPa compared to 2.1 kPa in Fig. 12f) due to the fixity provided by the continuous URM top support (see Fig. 5e). The effect of the applied overburden on wall AT was included when calculating the predicted wall behavior using the analytical method discussed earlier.

During test AT-A additional vertical, horizontal, and diagonal cracking occurred at the top corners of the tested wall strip. Re-testing the wall (AT-B) showed that wall stiffness and strength decreased, as reported in Fig. 12f. The curve representing test AT-B in Fig. 12f has been adjusted to exclude the inelastic deformations (about 15 mm) that occurred during test AT-A.

AT-Retrofitted

Due to the increased strength of the as-built wall resulting from continuity at the top support, from arching action, and from substantial additional axial load on the wall segment, the increase in flexural strength as a result of the NSM FRP strengthening was not pronounced, being only 27% as detailed in Table 5. The wall ductility capacity improved, with almost no reduction in wall strength as the wall displacement increased. However the wall exhibited 50 mm of residual displacement, which was equal to more than 35% of the maximum wall displacement as detailed in Table 5.

Wall WT (CB top support)

WT - As-built

A relatively stiff concrete beam that was cast above wall WT resulted in significant arching action, such that wall WT remained uncracked during test WT-A. Subsequently the wall was re-designated as WT-B and modified to have a pinned support condition that when re-tested resulted in wall cracking at a 3.2 kPa face pressure (Fig. 12g). Wall WT-A sustained a face pressure of more than 1.5 times the face pressure associated with wall cracking for WT-B when the top support concrete ring was cut (4.9 kPa compared to 3.2 kPa from Fig. 12g). Fig. 12h shows that the wall strength and the general shape of the behavioral curve dictating Δ_2 (see also Fig. 2) had a good correlation with the lab-based idealised model. The measured initial cracked wall stiffness was greater than the predicted equivalent, but as discussed previously the initial stiffness has an insignificant effect on the adopted displacement-based wall assessment (Griffith et al. 2003).

WT-Retrofitted

After being retrofitted, the strength of Wall WT-NSM FRP (5.6 kPa face pressure; see Fig. 12g) was 75% greater than that of the unretrofitted wall (3.2 kPa face pressure at cracking), and as detailed in Table 5, the improvement in wall strength due to the retrofit work was 830% when compared to the as-built maximum post-cracking strength (0.6 kPa). The wall behavior was ductile, and similar to the test on retrofitted wall AH1, the failure mode was characterized by cracking in the masonry substrate and debonding of the strip (Fig. 13a). Similar to tests on retrofitted walls AH1 and AH2, test WT–NSM FRP also resulted in a residual displacement in excess of 20 mm (more than 20% wall maximum displacement).

Investigation of the data presented in Fig. 12g suggests that the out-of-plane strength of wall WT with the as-built support details was approximately 1.2 times the seismic demand (NZS 1170.5:2004, NZS 2004) calculated for this wall configuration and site, being a region with high seismicity (Wellington, New Zealand). These test data suggest that constructing a bond beam in an existing building at the floor or roof levels is a reliable option for improving the out-of-plane seismic wall response. Fig. 12g also suggests that when the top concrete beam is absent, the same wall retrofitted using the NSM FRP technique meets the strength requirements for the region discussed, although wall loading will result in substantial residual displacement.

Table 6 details the uncracked and cracked wall stiffness data measured during the tests conducted on three one-way spanning walls and on the two-way spanning walls. The ratio of the cracked wall stiffness to the measured uncracked equivalent was found to be on average 0.34, but with large variation among the three walls (CoV=1.4). As a convention, a secant stiffness corresponding to two-thirds of the wall maximum force resistance was calculated from the post-cracking force-displacement curves and was assumed as the cracked wall stiffness. The ratio of the maximum wall face pressure before cracking, w_{cr}, to the residual wall face pressure after cracking, w_{max}, is notably high for several one-way spanning walls (see Table 6). This ratio varies from 250% to 530%, with the average value being 353%. This relatively high average percentage suggests that a study to show whether strength-based criteria for wall seismic assessment are more efficient compared to stability-based criteria is worthwhile, particularly for walls that have strong plaster finish and are located in regions with low seismicity.

Two-way spanning walls

Fig. 14a and Fig. 14b show the results of two-way spanning tests performed on damaged walls WH1 and WH2. Both walls underwent small amounts of inelastic deformation (approx. 0.5 mm, nearly 20% wall maximum displacement), with only minor additional cracking being developed.

Analysis of the response envelope shown in Fig. 14b indicated that at a face pressure of approximately 3.2 kPa the wall stiffness reduced by approximately 65% from 3.6 kPa/mm to 1.2 kPa/mm. This reduction in the wall stiffness was due to extension of the crack pattern as shown in Fig. 6. In contrast, WH1 maintained the same stiffness during testing, suggesting that the existing cracks did not open sufficiently to cause deterioration of wall stiffness. As discussed previously, the existing cracking in WH1 was not as extensive as that shown in Fig. 6 for WH2. The retrofit of WH2 using two strips of NSM FRP resulted in a 67% improvement in the wall stiffness, from 1.2 kPa/mm (WH2) to 2 kPa/mm (WH2-NSM FRP). Because the wall stiffness had improved and the wall resistance exceeded that required as per the NZ seismic loading requirements for regions with high seismicity, the test was terminated to avoid further wall damage. It should be noted that from the results of tests on the other retrofitted walls, the NSM retrofit method does not substantially improve wall stiffness, but instead the method significantly improves wall strength. The true effectiveness of the retrofit deployed for this strengthened two-way spanning wall could not be assessed due to the applied forces being insufficient to cause wall failure.

Fig. 15 shows a comparison between the force-displacement plots of unretrofitted wall WH3 and retrofitted wall WH4. Although the walls had identical dimensions and were merely located in different rooms, the flexural stiffness of WH4 (retrofitted) was 54% that of WH3 (as-built). Therefore the effectiveness of the retrofit work could not be established due to possible variation in material properties, construction details, e.g. the plaster thickness on each side, and due to potentially different extents of non-visible damage.

The measured wall stiffness during the tests on pre-cracked walls WH1 and WH2 was on average 2.9 kPa/mm, as detailed in Table 6. The measured wall stiffness during the tests on uncracked partition walls WH3 and WH4 was much higher than the measured value for the pre-cracked walls, despite the uncracked walls having larger wall dimensions. The average uncracked wall stiffness was 14.6 kPa, which was approximately 5 times greater than the average stiffness of the pre-cracked walls (2.9 kPa). This difference was attributed to two factors, one being prior cracking and the other being the unrestrained top horizontal edge in wall tests WH1 and WH2.

Although both walls WH1 and WH2 were pre-cracked, the maximum applied face pressure was approximately 30 times higher than that expected for a one-way spanning wall with the same thickness (calculated as 0.2 kPa using the procedure described in NZSEE (2006)). This comparison suggests that unnecessary retrofit measures can be avoided by utilising in-situ tests (C7.2.3.3.4 of ASCE 2007), although variability in wall stiffness, as shown in Fig. 15, should also be considered. Due to the substantial cost of conducting in-situ tests, this type of evaluation (including the required study into the variability of the results) is usually beneficial only when a large number of comparable walls exist in a masonry building.

SUMMARY AND CONCLUSIONS

A report of in-situ out-of-plane airbag testing that was conducted on as-built and retrofitted URM walls of four different buildings was presented. The test walls had plastered surfaces, and included one-way vertically spanning walls and uncracked or pre-cracked two-way spanning walls. The experimental program included testing the same walls with original and modified top support types.

A concrete ring beam positioned above URM bearing walls significantly increased wall strength and prevented excessive wall displacements. It was suggested that constructing bond beams at the floor or roof level of URM bearing wall buildings is a reliable seismic improvement option.

A single CFRP NSM strip or two inserted TSBs substantially increased the post-cracking out-of-plane flexural strength of one-way spanning walls AH1, AH2, AH3, AT, and WT by, respectively, 670%, 614%, 440%, 27%, and 830%. These increases in the wall strength were accompanied by residual displacements from nearly 20% and up to 35% of the wall maximum displacement. Therefore these retrofit techniques are recommended for ultimate limit state design where the functionality of the wall after a design earthquake is of limited importance. The behavior of a retrofitted wall that failed due to NSM FRP strip pull-out was brittle, but significant ductility was observed for walls where the NSM strip debonding failure mode was initiated. Consideration should be given in the NSM FRP seismic retrofit design to prevent the pull-out failure mode.

A previously cracked two-way spanning wall was tested in both as-built and NSM FFRP retrofitted conditions. The retrofit work improved the wall stiffness by 67%. No apparent improvement was observed when the stiffness of a retrofitted two-way spanning wall was compared to a different unretrofitted wall, potentially due to differences in the wall construction and/or different extents of prior non-visible wall damage. The complete effectiveness of the retrofit scheme for two-way walls could not be assessed due to the applied forces being insufficient to promote wall failure. It is also suggested based on this variability that individual wall boundary conditions, material properties, and previous loading history are required to be studied before a general seismic assessment procedure can be used.

The tested two-way spanning walls had strengths that were significantly greater than that calculated for a one-way spanning wall with the same thickness, but their out-of-plane stiffness was shown to be significantly reduced (by a factor of 5) due to cracking and/or due to the top wall edge being unrestrained. Irrespective of the results of wall assessment using procedures based on a one-way bending idealisation, even pre-cracked two-way spanning walls may satisfy current seismic loading standards. This study highlighted the merits of conducting in-situ testing as recommended by ASCE (2007) to assess wall strength, especially when a large number of comparable walls are involved and a desktop evaluation can potentially impose substantial unnecessary retrofit measures to be implemented in buildings. Significant variability was observed in the measured stiffness of two-way spanning walls of a single building, suggesting that multiple walls should be tested when a building is to be assessed by means of in-situ testing.

ACKNOWLEDGEMENTS

The authors wish to acknowledge the financial support provided by the New Zealand Government via the Foundation for Research Science and Technology (FRST). The authors also wish to acknowledge the financial support provided by the Australian Research Council (ARC).

REFERENCES

Abrams, D. P., Angel, R., Uzarski, J. (1996). "Out-of-plane strength of unreinforced masonry infill panels," Earthquake Spectra, EERI, 12(4):825-844.

ASCE (2007). Seismic Rehabilitation of Existing Buildings, ASCE/SEI 41-06. American Society of Civil Engineers, Reston, VA.

ASTM (2001). “Standard test method for measurement of masonry flexural bond strength.” C 1072 00a. ASTM International, Pennsylvania, United States.

ASTM. (2003). "Standard Test Methods for Sampling and Testing Brick and Structural Clay Tile." C 67-03a, ASTM International, Pennsylvania, United States.

ASTM (2004). “Standard test method for compressive strength of masonry prisms.” C 1314 03b. ASTM International, Pennsylvania, United States.

Calvi, G. M., Kingsley, G. R., and Magenes, G. (1996). “Testing of masonry structures for seismic assessment.” Earthquake Spectra, 12(1), 145–162.

Carpinteri, A., Invernizzi, S., and Lacidogna, G. (2005). “In situ damage assessment and nonlinear modelling of a historical masonry tower.” Engineering Structures, 27(3), 387–395.

Chiostrini, S., Galano, L., and Vignoli, A. (2003). “In situ shear and compression tests in ancient stone masonry walls of Tuscany, Italy.” Journal of Testing and Evaluation, 31(4), 289–303.

Corradi, M., Borri, A., and Vignoli, A. (2003). “Experimental study on the determination of strength of masonry walls.” Construction and Building Materials, 17(5), 325–337.

Derakhshan, H. (2012). “Seismic assessment of out-of-plane loaded unreinforced masonry walls” PhD thesis, Faculty of Engineering of The University of Auckland, New Zealand.

Derakhshan, H., Griffith, M., and Ingham, J. (2013). “Out-of-plane behavior of one-way unreinforced masonry walls.”, ASCE Journal of Engineering Mechanics, 139, 4, 409-417.

Downes, G., Dowrick, D., Van Dissen, R., Taber, J., Hancox, G., & Smith, E., (2001). The 1942 Wairarapa, New Zealand, earthquakes; analysis of observational and instrumental data, Bull. of the N.Z. Soc. for Earthquake Engineering, 34, 125-157.

Doherty, K. T. (2000). “An investigation of the weak links in the seismic load path of unreinforced masonry buildings,” PhD thesis, Faculty of Engineering of The University of Adelaide, Australia.

Griffith, M. C., Magenes, G., Melis, G., and Picchi, L. (2003). Evaluation of out-of-plane stability of unreinforced masonry walls subjected to seismic excitation. Journal of Earthquake Engineering, 7(SPEC. 1):141–169.

Griffith, M.C. , Kashyap, J. , Mohamed Ali, M.S. (2013). Flexural displacement response of NSM FRP retrofitted masonry walls. Article in Press (DOI: 10.1016/j.conbuildmat.2012.06.065).

Hamed, E., Rabinovitch, O. (2010). Failure characteristics of FRP-strengthened masonry walls under out-of-plane loads. Engineering Structures, 32(8): 2134-2145.

Kashyap, J., Willis, C.R., Griffith, M.C. , Ingham, J.M., Masia, M.J. (2012). Debonding resistance of FRP-to-clay brick masonry joints. Engineering Structures, 41: 186-198.

Lumantarna, R., Biggs, D. T., and Ingham, J. M. (2013). "Compressive, Flexural Bond and Shear Bond Strengths of In-Situ New Zealand Unreinforced Clay Brick Masonry Constructed Using Lime Mortar between the 1880s and 1940s." J. Mater. Civ. Eng., 10.1061/(ASCE) MT.1943-5533.0000685 (Sep. 18, 2012).

NZSEE (2006). “Assessment and Improvement of the Structural Performance of Buildings in Earthquake. Recommendations of a New Zealand Society for Earthquake Engineering Study Group on Earthquake Risk Buildings”. Wellington, New Zealand.

Priestley, M. J. N. (1985). “Seismic behavior of unreinforced masonry walls.” *Bulletin of the New Zealand National Society for Earthquake Engineering*, 18(2), 191–205.

Vaculik, J. (2012) Unreinforced Masonry Walls Subjected to Out-of-Plane Seismic Actions. PhD Thesis, University of Adelaide.

LIST OF TABLES

TABLES

TABLE 1: Wall properties

Wall	Test span condition	Thickness[1]	Height	Length	Plaster[2] thickness		Masonry unit dimensions (mm)
		t_n (mm)	h (mm)	l (mm)	t_{p1} (mm)[3]	t_{p2} (mm)[4]	
AH1	One-way	150	3300	1170	20[5]	20[5]	68 × 230 × 112
AH2	One-way	150	3300	1170	20[5]	20[5]	
AH3	One-way	270	2700	1200	20[5]	10	
AT	One-way	240	3000	1200	---	10	75 × 220 × 105
WT	One-way	255	4000	1250	15	15	75 × 220 × 105
WH1	Two-way	130	2730	3850	15	15	160 × 300 × 95
WH2	Two-way	130	2730	3480	15	15	
WH3	Two-way	130	2940	4100	15	15	
WH4	Two-way	130	2940	4100	15	15	

Notes - (1) Including plaster (2) Cement-based plaster unless indicated otherwise (3) Loaded wall face (4) Other wall face (5) Lime-based plaster

TABLE 2: Material properties

Bldg	Half-brick compressive strength, f_b' (MPa) ASTM C67– 03a (ASTM 2003)	Mortar compressive strength, f_j' (MPa)	Masonry compressive strength, f_m' (MPa) ASTM C 1314-03b (ASTM 2004)	Plaster compressive strength, f_p' (MPa)	Masonry flexural bond strength, f_{fb}' (MPa) C 1072 00a ASTM (2001)
	(No. of samples) Mean (CoV)				
AH	(7) 8.8 (0.19)	(8) 3.3 (0.37)	(5) 3.2 (0.2)	(9) 1.4 (0.37)	(9) 0.04 (0.5)
AT	(9) 19.4 (0.16)	(9) 5.7 (0.28)	(6) 9.6 (0.28)	N/A	N/A
WT	(5) 25.9 (0.25)	(6) 17.7 (0.46)	(5) 9.7 (0.18)	N/A	(2) 0.61 (N/A)
WH	(3) 32* (0.26)	N/A	(4) 13.8* (0.5)	(7) 3.4 (0.15)	N/A

* Compressive strength results are based on net block area

TABLE 3: In-situ as-built testing program

Wall	Span Condition	Test	Wall support		
			Top	Bottom	Conditions
AH1	One-way	A	SA	Ground	O
	One-way	B	TD	Ground	M
AH2	One-way	A	TD	Ground	M
AH3	One-way	A	G	Ground	M
AT	One-way	A	C	C	O
	One-way	B	CC	C	M
WT	One-way	A	CB	Ground	O
	One-way	B	TD	Ground	M
WH1	Two-way	A	U	CB	O
WH2	Two-way	A	U	CB	O
WH3	Two-way	A	CB	CB	O
WH4	Two-way	A	CB	CB	R

Notes - O: Original; M: Modified; C: Continuous; TD: Timber Diaphragm CC: Cracked Continuous; CB: Concrete Beam; SA: Steel Anchor; G: Gap; U: Unrestrained, R: Retrofitted

TABLE 4: In-situ retrofitted wall testing program

Test	d_f (mm)	b_f (mm)	b_p (mm)	t_p or d_b (mm)	# of NSM Bar/strip	S_v (mm)
AH1-NSM FRP	35	8	15	1.2	1	1170
AH2-NSM TSB	30	10	---	6	2	585
AH3-NSM FRP	25	6	15	1.2	1	1200
AT-NSM FRP	25	6	15	1.2	1	1200
WT-NSM FRP	20	6	15	1.2	1	1250
WH2-NSM FRP	30	5	15	1.2	2	1200
WH4-NSM FRP	30	5	15	1.2	2	1200

d_f = width of groove; b_f = depth of groove; b_p = width of FRP strip; t_p = thickness of FRP strip; d_b = outer diameter of TSB; and Sv = centre to centre spacing of vertical bars/strips

TABLE 5: In-situ retrofitted wall test results

Wall	Post cracking as-built face pressure (kPa)	Retrofitted maximum achieved face pressure (kPa)	Retrofit strength improvement (%)	Residual disp. as a percentage of max. disp. (%)
AH1	0.18	1.4	670	20
AH2	0.14	1.0	614	20
AH3	0.90	4.9	440	---**
AT	4.10	5.2	27	35
WT	0.60	5.6	830	20
WH2	4.90	5.9	N/A*	20
WH4	3.80	3.80	N/A*	---***

* The true effectiveness of the retrofit is not evident due to test termination; ** brittle failure; *** elastic behavior

TABLE 6: In-situ as-built test results

Test	K_{uc}	K_{cr}	K_{cr}/K_{uc}	w_{cr}	w_{max}	w_{cr}/w_{max} x100
	(kPa/mm)			(kPa)	(kPa)	(%)
One-way walls						
AH1-A	0.43	0.02	0.05	0.5	0.2	250
AH3-A	0.64	0.56	0.88	2.5	0.9	280
WT-B	1.3	0.12	0.09	3.2	0.6	530
Average (CoV)			0.34 (1.4)			353 (0.4)
Two way walls						
WH1-A		2.3				
WH2-A		3.5				
WH3-A	18.9					
WH4-A	10.3					
Average	14.6	2.9				

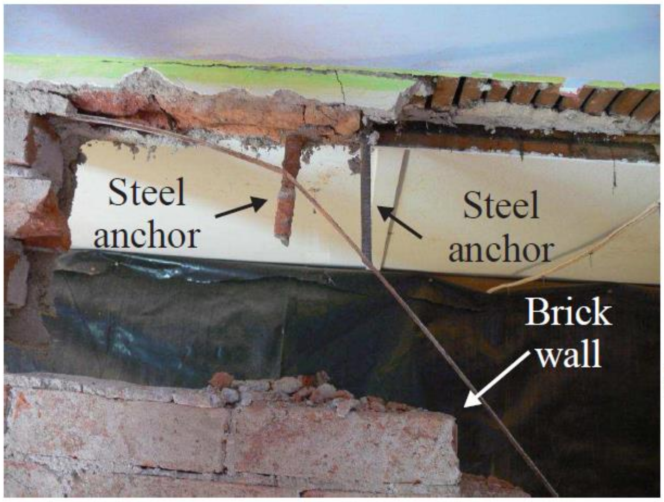

(a) Steel anchors in demolished wall

(b) Anchorage details

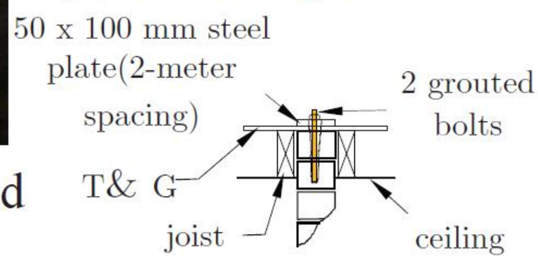

(c) Anchorage sketch

Fig. 1: Grouted steel anchors (SA)

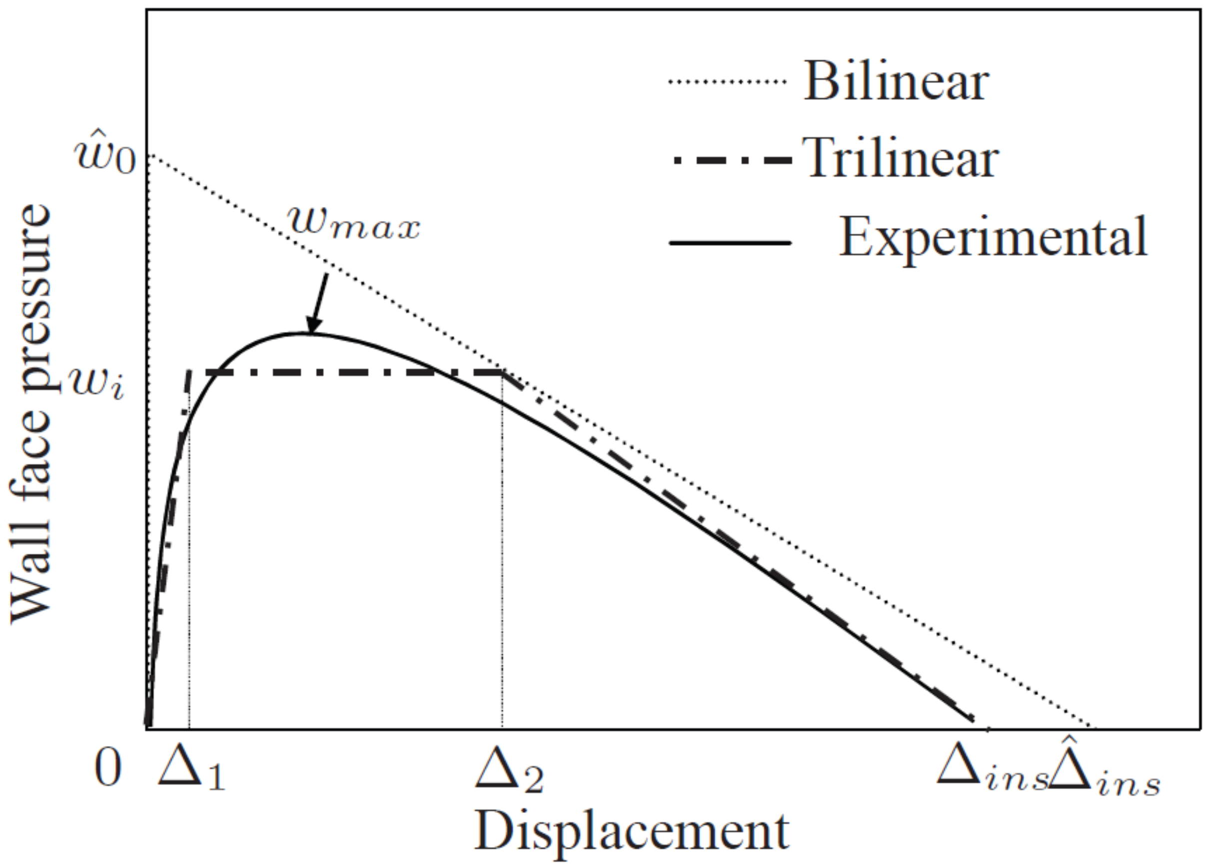

Figure 2: Wall out-of-plane behaviour

(a) Avon House (b) Allen's Trade Complex (c) Wintec F Block (d) William Weir House (facing S-E)

Fig. 3: Case study buildings

(a) AH (b) AT and WT (c) WH

Fig. 4: Typical wall cross section

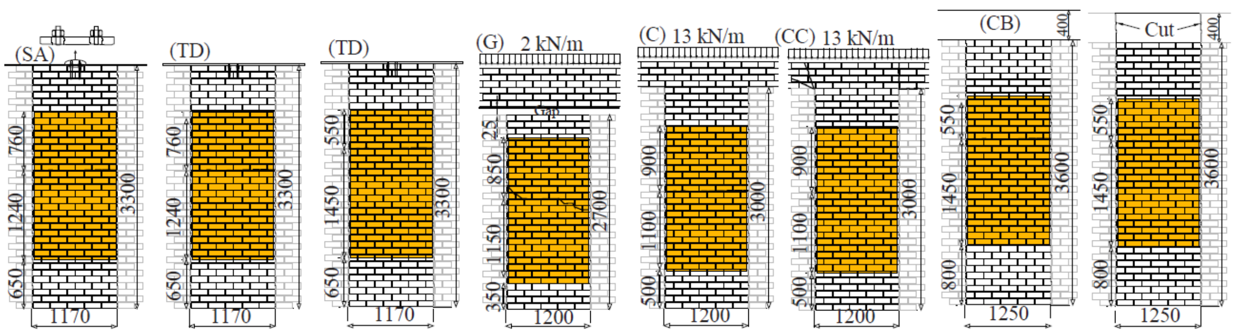

(a) AH1-A (b) AH1-B (c) AH2-A (d) AH3-A (e) AT-A (f) AT-B (g) WT-A (h) WT-B

Fig. 5: Dimensions and boundary conditions of one-way vertically spanning walls; thick black lines indicate wall cracks; shaded area indicates the position of airbags; refer to Table 3 for details of boundary support codes

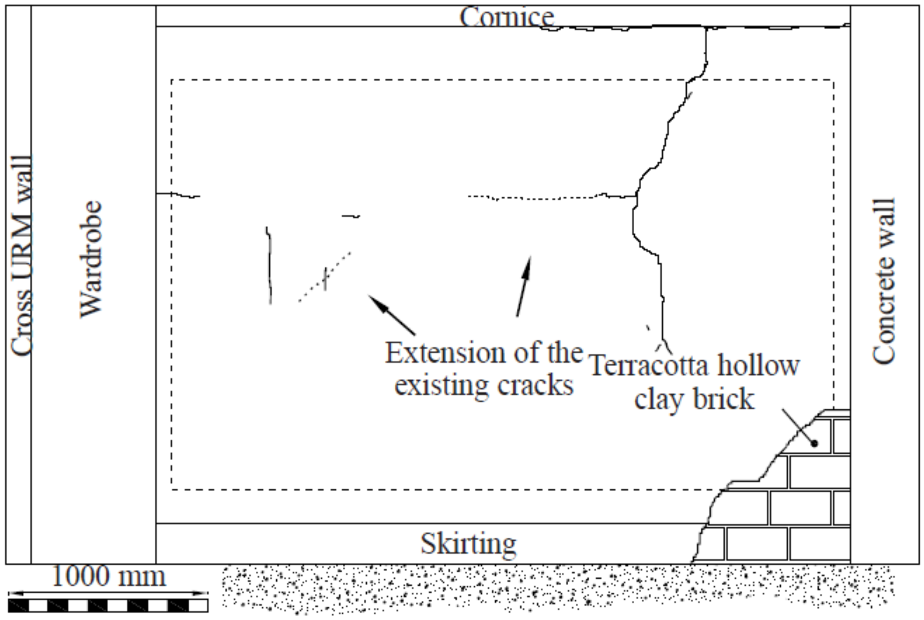

658 Fig. 6: Wall WH2 initial crack pattern and crack extension (dashed)

(a) Wall cross section (b) Wall disintegration

Fig. 7: Scarcity of header bricks in a two-leaf wall

(a) Masonry prism testing (b) Four-point bending test

Fig. 8: Material testing on building WH

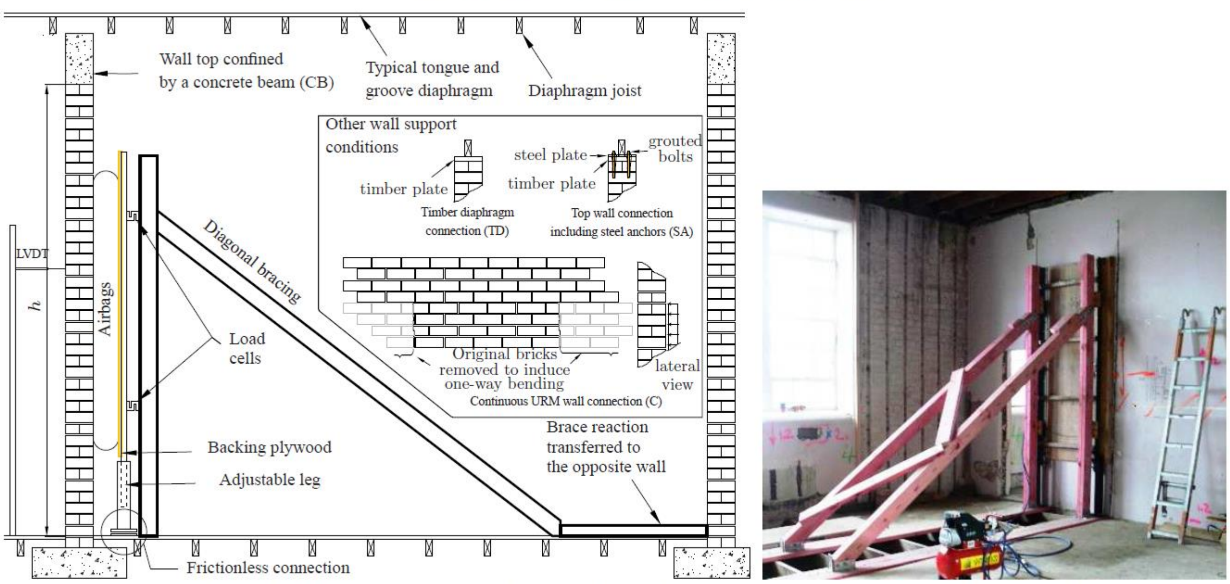

(a) Test setup diagram for WT-A; inset: top support details for other walls (b) Actual setup (WT-A)

Figure 9: Typical in-field test setup details

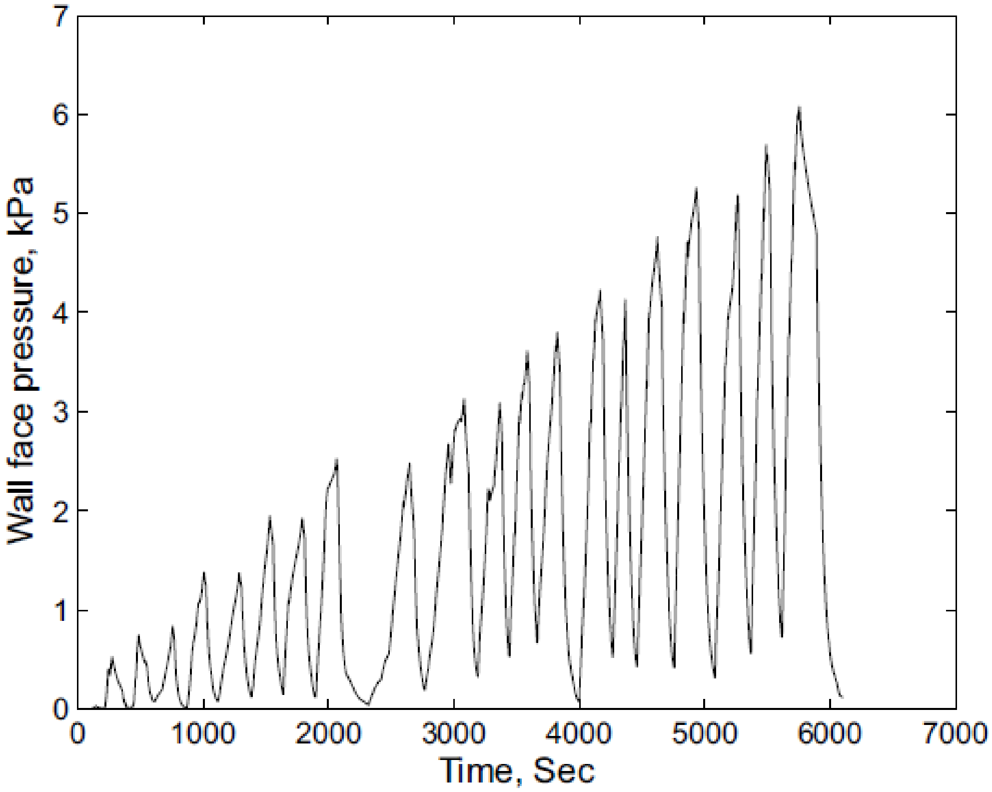

Fig. 10: Recorded loading history (from test WH2)

(a) Horizontal crack (WT-B)

(b) Plaster crushing (AH2-B)

(c) Plaster debonding (AH1-A)

(d) Crack pattern in a retrofitted wall (AH1-NSM FRP)

Fig. 11: Wall cracking and deterioration of plaster

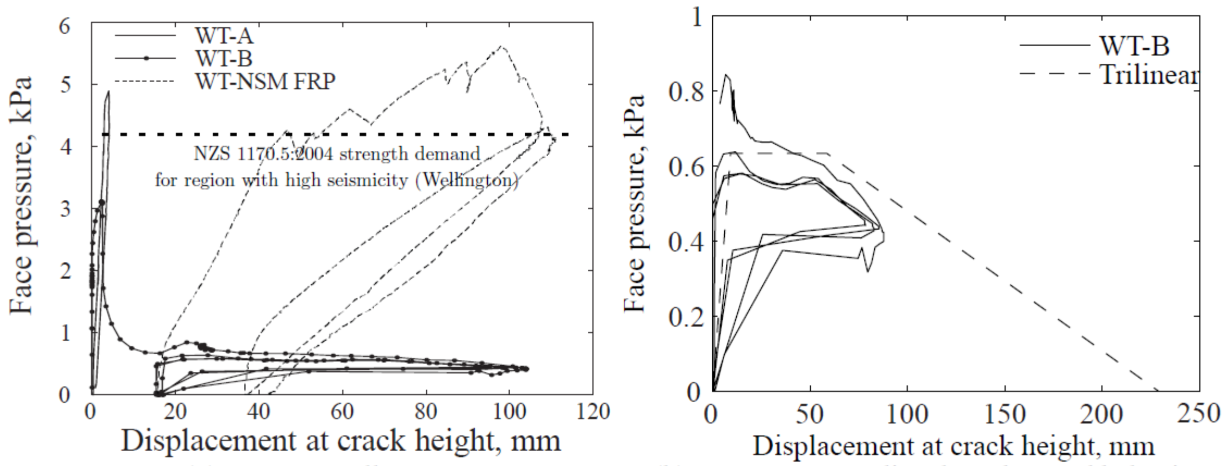

(g) Tests on wall WT (h) Test WT-B; predicted vs observed behavior

FIG. 12: Face pressure-lateral displacement relationship-Contd.

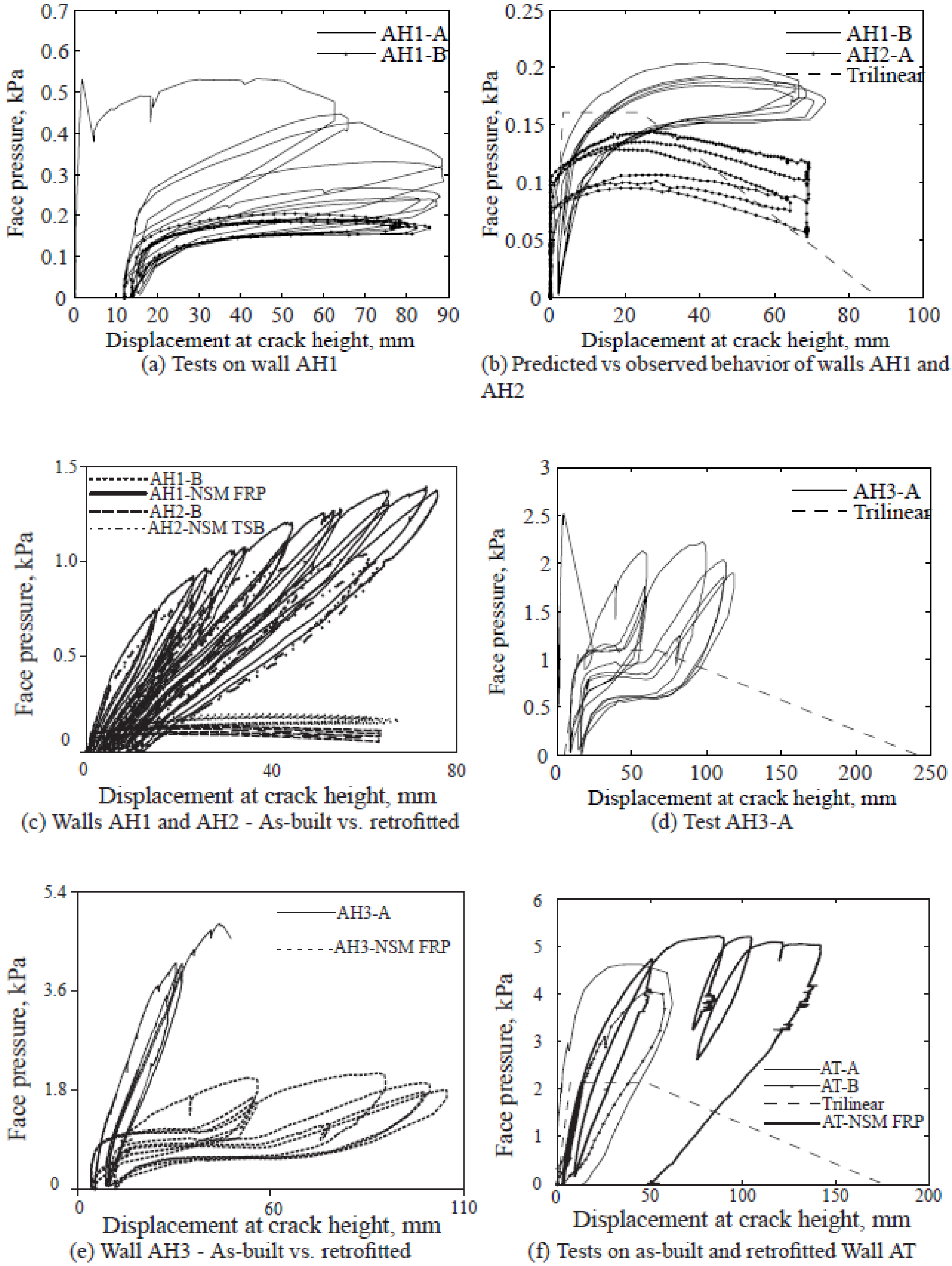

(a) Tests on wall AH1

(b) Predicted vs observed behavior of walls AH1 and AH2

(c) Walls AH1 and AH2 - As-built vs. retrofitted

(d) Test AH3-A

(e) Wall AH3 - As-built vs. retrofitted

(f) Tests on as-built and retrofitted Wall AT

FIG. 12: Face pressure-lateral displacement relationship

(a) Strip debonding (WT – NSM FRP)

(b) Strip pull-out (AH3 – NSM FRP)

(c) Local bending of a TSB (AH2 – NSM TSB)

Fig. 13: Failure modes in retrofitted walls

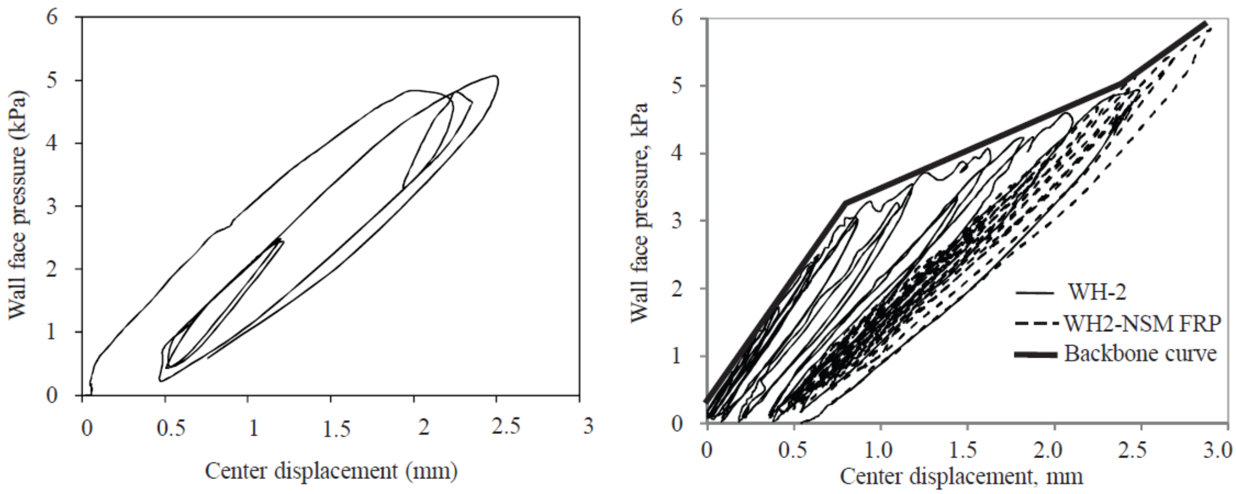

(a) Test WH1-A

(b) Tests WH2-A and WH2-NSM FRP

FIG. 14: Results of tests on WH1 and WH2

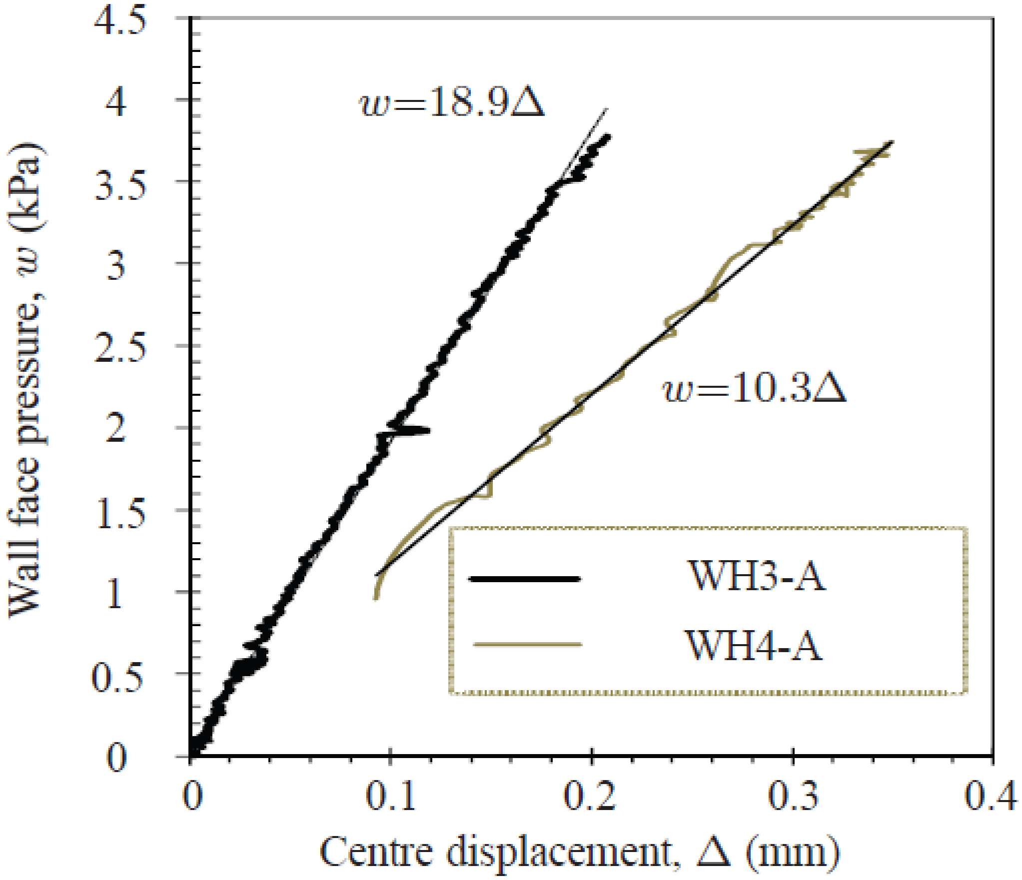

668 Fig. 15: Results of tests on WH3 and WH4